An X-ray and Neutron Scattering Study of the Structure of Zinc Vanadate Glasses

Uwe Hoppe, Rainer Kranold, Emil Gattef[a], Jörg Neuefeind[b], and David A. Keen[c]

Universität Rostock, Fachbereich Physik, D-18051 Rostock
[a] University of Chemical Technology & Metallurgy, 1756 Sofia, Bulgaria
[b] Hamburger Synchrotronstrahlungslabor HASYLAB am Deutschen Elektronensynchrotron DESY, Notkestr. 85, D-22607 Hamburg
[c] ISIS Facility, Rutherford Appleton Laboratory, Chilton, Didcot, OX11 0QX, UK

Reprint requests to Dr. U. H.; Fax: +49 381 4981726, E-mail: Hoppe@physik1.uni-rostock.de

Z. Naturforsch. **56a,** 478–488 (2001); received April 3, 2001

The short-range order of vitreous V_2O_5 and of three $(ZnO)_x(V_2O_5)_{1-x}$ glasses with $x = 0.2$, 0.4, and 0.5 is studied by X-ray and neutron diffraction experiments where the change of the contrast allows to resolve the V–O and Zn–O correlations. The V–O and the Zn–O first-neighbor peaks are approximated by several Gaussian functions. In case of vitreous V_2O_5 two obvious V–O distances exist which are related with VO_4 and VO_5 units. With ZnO additions the V–O coordination number decreases from 4.4 in vitreous V_2O_5 to 4.0 in the metavanadate glass where the strongest decrease of the fraction of VO_5 units is found for glasses of $x < 0.2$. Dominantly, the VO_5 groups are linked with the neighboring units by corners. The Zn-O coordination numbers of the modified glasses are about five with closest distances of $\cong 0.200$ nm.

Key words: Neutron Scattering; X-ray Scattering, Short-range Order; Vanadate Glasses.

1. Introduction

The vanadate glasses belong to those oxydic materials whose structures have been investigated only rarely. Though $(MeO)_x(V_2O_5)_{1-x}$ glasses with typical network-modifiers MeO, such as the alkaline earths, can be prepared by rapid quenching in a wide compositional range from $x \cong 0.1$ to $x < 0.5$, and though vanadium atoms are good scatterers of X-rays, systematic diffraction studies of such materials do not exist. The glasses are known as semiconducting materials whose property is due to the coexistence of two valence states, V^{4+} and V^{5+}, of the vanadium ions [1, 2]. The electrical conductivity is based on the hopping of an unpaired $3d^1$ electron from a V^{4+} to a V^{5+} site [3]. In alkaline earth vanadate glasses the V^{4+} cations exist in fractions of about 5% and less, such as found, e.g., in Mg and Sr vanadate glasses [4, 5]. Thus, in a first approach the V^{4+} ions can be neglected in the structural analysis, and a binary glass with the stoichiometric formula $(MeO)_x(V_2O_5)_{1-x}$ can be assumed. When these glasses are compared with others, first one remembers those of P_2O_5. Since vanadium and phosphorus have the same valency, one would expect some common features in the structures. The vanadate crystals show some structural forms being similar to those of the phosphates. Chains formed of corner-linked VO_4 tetrahedra exist in the $Ba(VO_3)_2$ crystal [6]. They are similar to the chains of PO_4 units found in the polyphosphates. But different from the phosphates formed of only PO_4 units, also larger VO_n polyhedra occur. Edge-connected VO_5 units form zig-zag chains in crystalline (c–)V_2O_5 [7] and in c–$Zn(VO_3)_2$ [8]. In c–V_2O_5 the chains are interconnected to layers. With increasing fractions of the modifier oxide, however, the vanadium tends to form VO_4 tetrahedra. With further ZnO additions also such units occur. The pyrovanadate V_2O_7 groups in c–$Zn_2V_2O_7$ [9] are pairs of corner-linked VO_4 tetrahedra.

What is already known about the structure of the vanadate glasses? By ^{51}V nuclear magnetic resonance (NMR) spectroscopy of some alkaline-earth vanadate glasses [10] the depolymerization process was studied which occurs along with MeO additions. This process obeys a similar scheme of breakage of V–O–V bridges between the VO_4 units as known of the PO_4 units in the phosphate glasses [11]. At metavanadate composition ($x = 0.5$), chains of corner-linked VO_4 units dominate. But additionally, the more one approaches vitreous (v–)V_2O_5, a clear fraction of VO_5 units occurs. Similar changes from networks of VO_5 units in v–V_2O_5 to chains of VO_4 units at metavanadate composition were found by infrared (IR) spectroscopy [12]. For the V_2O_5 glass a layer-like structure similar to that of c–V_2O_5 [7] was suggested [12]. On the basis of X-ray diffraction

0932-0784 / 01 / 0600-0478 $ 06.00 © Verlag der Zeitschrift für Naturforschung, Tübingen · www.znaturforsch.com

(XRD) work, other authors [13] suggested a network structure formed of VO_4 tetrahedra similar to that of v–P_2O_5, which idea is in line with the results obtained for the V_2O_5 melt [14]. Molecular Dynamics (MD) simulations of v–V_2O_5 yield a model which is dominated by corner-linked VO_5 units having no terminal V–O bonds [15]. According to our XRD measurements using Ag K_α radiation we favoured [15] the network model from the MD simulations [15], though the V–O bond from XRD appears a little shorter than that from MD. A subsequent reverse Monte Carlo (RMC) analysis of our XRD data [16] leads to mixtures of corner-linked VO_5 and VO_4 units [17]. As a consequence, a reasonable fraction of terminal V–O bonds occurs [17]. Note that ^{51}V NMR spectroscopy of v–V_2O_5 [18] has also preferred the concept of a mixture of VO_5 and VO_4 units. The situation of knowledge is already controversial for v–V_2O_5 and even less details are known of the modified vanadate glasses.

In the present work our previous XRD measurements of v–V_2O_5 using Ag K_α radiation [16] are repeated for a larger Q-range using the high-energy photons from a synchrotron (Q is the magnitude of the scattering vector with $Q = 4\pi/\lambda \sin\theta$, λ is the radiation wavelength and 2θ is the scattering angle). Details of the V–O first-neighbor peak may become visible. The good resolving power should also help to separate the V–O and Me–O first-neighbor distances of the glasses, here modified by ZnO. The small series of vanadate glasses with ZnO fractions of 0.0, 0.2, 0.4 and 0.5 should give some first ideas of the effects of modifier additions. Neutron diffraction (ND) experiments are involved to increase the available information. The vanadium atoms have a very small coherent scattering cross-section for neutrons and, thus, the V–O correlations cause a very weak scattering contribution. Though the ND data are clearly dominated by the O–O correlations, they also corroborate the information about the Zn–O correlations. Thus, the combination of diffraction experiments allows to characterize the oxygen environments of the Zn^{2+} ions. Remember the behavior of the Zn–O coordination numbers, N_{ZnO}, in phosphate glasses $(ZnO)_x(P_2O_5)_{1-x}$, where N_{ZnO} varies with the compositions x [19, 20]. N_{ZnO} is six for $x \cong 0.3$, and it decreases to four at the metaphosphate composition ($x = 0.5$). Also the Zn–O distances decrease and approach 0.195 nm in the metaphosphate glass [19]. The changes were attributed to effects of a change of the number of terminal oxygen (O_T) atoms available for coordination of each Me site [19–21]. It arises the question whether a similar mechanism exists in the vanadate glasses.

Since we do not know any other series of vanadate glasses investigated by diffraction, only simple attempts can be made to understand the mechanism of a change of the VO_n polyhedra and the behavior of the medium-range order. A more thorough analysis will be possible after some modelling work. Here we can compare the structural behavior of the vanadate glasses with those of other glasses where the effects are better understood. The phosphate glasses are already mentioned where, however, due to small P–O distances, r_{PO}, of 0.155 nm [19], N_{PO}'s larger than four do not occur. On the other hand, the mean r_{VO}'s of more than 0.17 nm (0.172 nm in c–$Ba(VO_3)_2$ [6]) are similar to the r_{GeO}'s of about 0.175 nm in the GeO_4 units of the germanate glasses [22]. For these glasses, a change of N_{GeO} due to modifier additions is known [22] but N_{GeO} is four in v–GeO_2, and an increase is observed with alkali additions. The concerning part of the discussion is limited to qualitative remarks.

2. Experimental

2.1. Sample Preparation

The samples were prepared from powdered reagent grade ZnO and V_2O_5. Batches of 5 g of mixtures of $(ZnO)_x(V_2O_5)_{1-x}$ were melted in platinum crucibles in the temperature range 800–1200 °C for 15 min in air. The melts were quenched very rapidly to room temperature by twin-roller techniques. Cooling rates of up to 10^5 K/s are realized. The samples with $x = 0.2$ and 0.4 are completely amorphous, while v–V_2O_5 and the metavanadate sample have small crystalline fractions.

2.2. Diffraction Experiments

The XRD experiments were performed on the BW5 wiggler beamline at the DORIS III synchrotron (Hamburg/Germany). The samples with $x = 0.2$ and 0.4 were measured with an energy of 130 keV ($\lambda = 0.00954$ nm) of the incident photons, the other two samples were measured in a later experimental run with photon energies of 120.7 keV ($\lambda = 0.010272$ nm). The powdered sample material was loaded into silica capillaries of 2.0 mm diameter and with a wall thickness of 0.01 mm. During the measurements the specimens were positioned in a vacuum vessel to suppress air scattering. Since the scattering angles are small, the transmission factors are assumed to be independent of the angle. The angular increment in the step-scan mode was 0.05°. In the 2θ-

range from 0.35° to 9° an absorber was set in the diffracted beam to avoid counting rates higher than 10^5 s^{-1}. The other scans range from 8° to 25°. Details of such experiments and the corrections are described in [23]. The electronic energy window of the solid-state Ge-detector was chosen to pass the elastic line and the full Compton profile, but no fluorescence scattering. The dead-time corrections were made with $\tau = 2.4$ μs. A fraction of 0.91 of the incident photons is polarized horizontally. Both numbers allow to merge the data of the scans obtained for both angular ranges and with different synchrotron currents. Corrections are made for background, container scattering, and absorption. The scattering intensities are normalized to the structure-independent scattering functions which have been calculated by polynomial fits of the tabulated atomic parameters of the elastic and the Compton scattering data [24]. Finally, the Compton fractions are subtracted and Faber-Ziman structure factors, $S_X(Q)$, are calculated [25].

The ND experiments of the same samples were performed on the time-of-flight instrument SANDALS of the pulsed neutron source ISIS at the Rutherford Appleton Laboratory. The powdered material was loaded into thin-walled vanadium cylinders of 5 mm diameter and with a wall thickness of 0.025 mm. Due to the limitations of the available sample material the beam height was reduced to 1 cm. The absorption and multiple scattering corrections are made by the ATLAS program suite [26]. The self scattering contributions are calculated according to the compositions of the samples, where the inelasticity effects are small due to the small scattering angles of SANDALS. The scattered intensities recorded in the various detector groups and normalized to separate self terms are merged to the differential scattering cross-section. Due to the small quantities of the samples and the limitations in the measuring time, the data beyond 200 nm^{-1} are already very noisy. However, since mainly Zn–O and O–O correlations dominate the ND data, not much information is expected at higher Q. Finally, the incoherent scattering is subtracted and total neutron structure factors, $S_N(Q)$, are calculated [25].

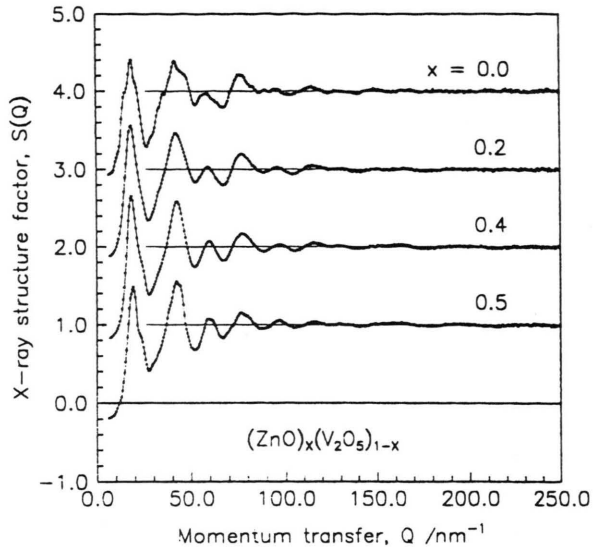

Fig. 1. X-ray structure factors, $S(Q)$, of v–V_2O_5 and of three zinc vanadate glasses with ZnO fractions, x, of 0.2, 0.4 and 0.5. The little Bragg peaks in the lower and the upper functions evidence for small crystalline fractions in these samples (cf. also Figure 2). The upper functions are shifted for clarity.

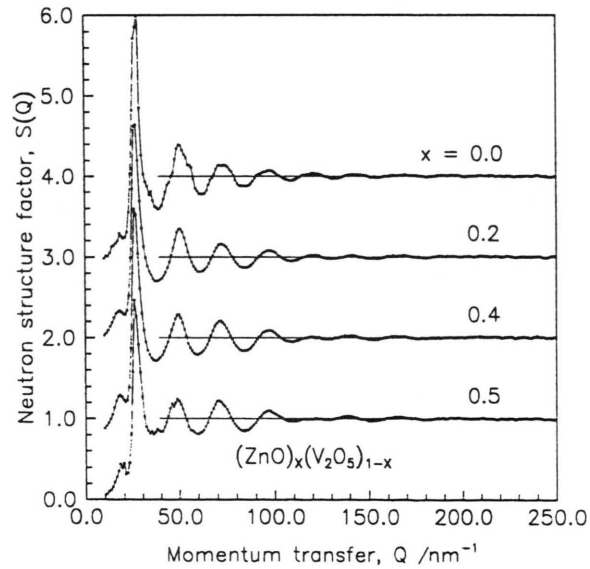

Fig. 2. Neutron structure factors, $S(Q)$, of v–V_2O_5 and of zinc vanadate glasses with ZnO fractions, x, of 0.2, 0.4, and 0.5. The upper functions are shifted for clarity.

3. Results

The structure factors $S_X(Q)$ and $S_N(Q)$ of the four samples measured are shown in Figs. 1 and 2, respectively. Due to the use of high-energy photons, the $S_X(Q)$ functions are available up to 280 nm^{-1} but the noisy data beyond 250 nm^{-1} show some unrealistic features and are not used. As to a small contamination with crystalline fractions, small Bragg reflections are visible in the $S_X(Q)$ and $S_N(Q)$ functions of v–V_2O_5 and the metavanadate

sample. Such small contributions only little affect that structural information which is extracted for the corresponding glasses. The variations visible in the $S(Q)$ data according to the ZnO additions are small. Especially the $S_N(Q)$ data do not much change, because the O–O edges of the VO_n polyhedra dominate the scattering. Thus, the first main maximum at 27 nm^{-1} in the $S_N(Q)$ data belongs to the O–O correlations, and it reflects a "packing" of the larger oxygen anions in the network of this oxide glass. Taking into account the strong scattering of the V and Zn atoms for X-rays, the O–O correlations play only a minor role in the XRD data. The maximum at $\cong 27$ nm^{-1} is not visible in the $S_X(Q)$ data. Here, the first maximum, which is seen only as a prepeak in the $S_N(Q)$ data, lies at $\cong 18$ nm^{-1}, and it reflects the "packing" of the VO_n and ZnO_n polyhedra.

The information in the short-range order is extracted from the correlation functions, $T(r)$, by peak fitting procedures. The correlation functions are obtained from the $S(Q)$ data by Fourier transformation (FT) with

$$T_k(r) = 4\pi r \varrho_0 + 2/\pi \int_0^{Q_{max}} \cdot Q \cdot [S_k(Q) - 1] \sin(Qr)\, dQ, \quad (1)$$

where ϱ_0 is the number density of atoms. No damping was applied in the FT procedure. The subscript k is either X or N for the XRD and ND data. The number densities used are calculated from mass densities published in [4, 13]. Thus, $\varrho_0 = 68.8$ nm^{-3} is used for v-V_2O_5 [13] and $\varrho_0 = 69$ nm^{-3} is used for the other glasses. The latter value is obtained from the mass densities of a series of Mg vanadate glasses [4]. Mg and Zn have similar dimensions, which justifies this choice. The resulting $T(r)$ data are shown in Figs. 4 and 5 in comparison with the final fitting results. The Q_{max}'s used in the FT procedure are indicated in the plots. The X-ray $T(r)$ functions (cf. Fig. 4) show asymmetric V–O peaks at 175 nm. For the glasses with 40 and 50 mol% ZnO the Zn–O correlations at 0.20 nm become evident. The O–O distances at 0.28 nm yield a rather small peak, while the large peak of the V–V and Zn–V distances at 0.34 nm increases with ZnO additions. Especially for v-V_2O_2 and the metavanadate glass some spurious oscillations exist below 0.1 nm. Both samples were measured in the same later run (cf. Chapter 2.2) where, obviously, some small systematic errors could not be eliminated. The main feature of the neutron $T(r)$ functions (cf. Fig. 5) is the O–O peak at 0.28 nm. The Zn–O peak at 0.20 nm increases with the ZnO fraction. The V–O peak at 0.175 nm yields a very small negative contribution in front of the Zn–O peak.

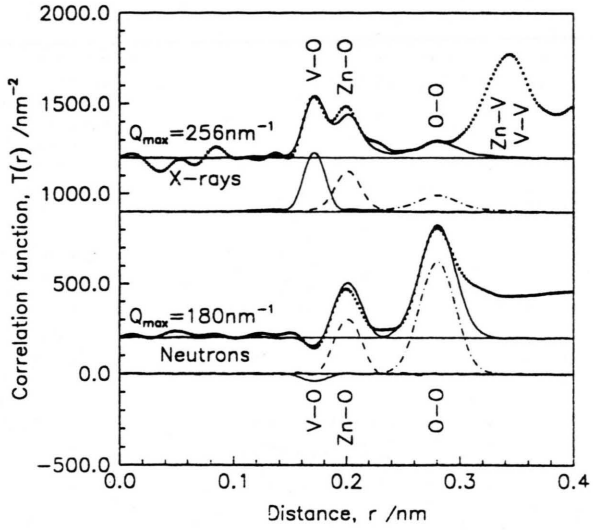

Fig. 3. Imperfect fit of the experimental X-ray and neutron correlation functions, $T(r)$, of the $(ZnO)_{0.5}(V_2O_5)_{0.5}$ glass (dotted lines) with some model functions (solid lines) where the V–O and Zn–O first-neighbor peaks are approximated by single Gaussian functions. The partial contributions given are broadened according to the effects of Q_{max} in the Fourier transformations: V–O (thin solid lines), Zn–O (dashed lines), O–O (dash-dotted lines). The upper functions are shifted for clarity.

Parameters of the V–O, Zn–O and O–O first-neighbor peaks are extracted by Gaussian fitting. The effects of the truncation at Q_{max} of the $S(Q)$ data used in the FT procedures are taken into account by a method described in [27], where in case of the X-ray data also the Q-dependent weighting factors are introduced. For fitting the $T(r)$ data, the Marquardt algorithm [28] is used where coordination numbers, mean distances and full widths at half maximum (fwhm) are the parameters of the model Gaussian functions. The fits of the XRD and ND $T(r)$ data are performed simultaneously. In a first approach, the three distance peaks are approximated by single Gaussian functions. The result for the zinc metavanadate glass is shown in Fig. 3, which shows that this model cannot be fitted successfully to the experimental data. The resulting fit parameters are given in Table 1, where also the small V–O coordination number of 3.5 differs from the expected number of four or more. Therefore, a more sophisticated approach must be applied. Three and two Gaussian functions are used for the V–O and Zn–O peaks, respectively, where the distance and fwhm parameters of the third and second contributions are fixed to

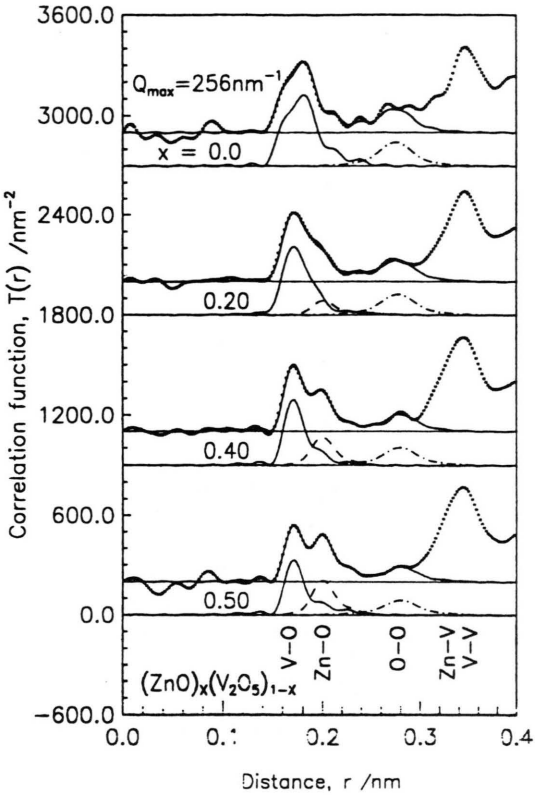

Fig. 4. Experimental X-ray correlation functions, $T(r)$, (dotted lines) in comparison with the model $T(r)$ functions (solid lines) fitting the V–O, Zn–O and O–O first neighbor peaks. The partial contributions given are broadened according to the effects of Q_{max} in the Fourier transformations: V–O (thin solid lines), Zn–O (dashed lines), O–O (dash-dotted lines). The upper functions are shifted for clarity.

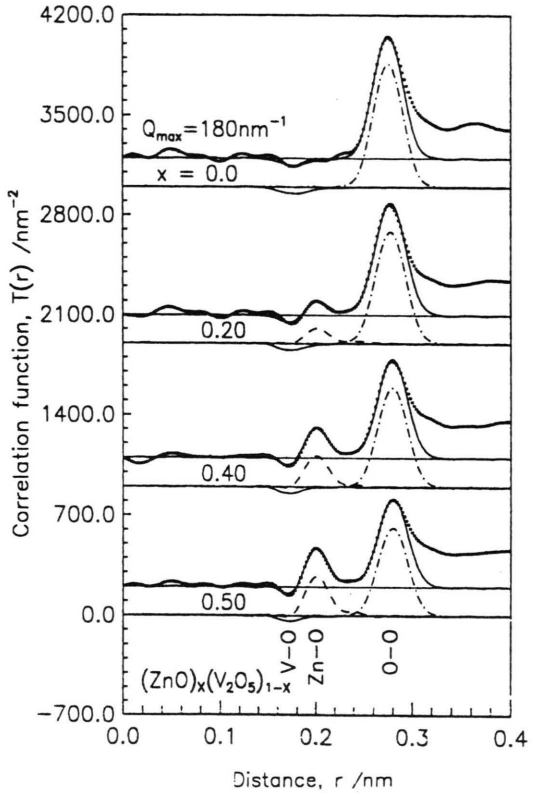

Fig. 5. Experimental neutron correlation functions, $T(r)$ (dotted lines) in comparison with the model $T(r)$ functions (solid lines) fitting the V–O, Zn–O and O–O first neighbor peaks. The partial contributions given are broadened according to the effects of Q_{max} in the Fourier transformations: V–O (thin solid lines), Zn–O (dashed lines), O–O (dash-dotted lines). The upper functions are shifted for clarity.

Table 1. Parameters resulting from an imperfect Gaussian fit of the experimental X-ray and neutron correlation functions, $T(r)$, of the $(ZnO)_{0.5}(V_2O_5)_{0.5}$ glass (cf. Fig. 3) where the V–O and Zn–O first neighbor peaks have been approximated by single Gaussian functions.

Atom pair	Coordin. number	Distance (in nm)	fwhm (in nm)
V–O	3.49	0.1715	0.022
Zn–O	4.73	0.2015	0.026
O–O	5.96	0.2805	0.037

equal each other (cf. Table 2). For the V–O peak of v–V_2O_5 even a small fourth Gaussian has to be introduced whose parameters are chosen somewhat arbitrarily. The excellent fit of the experimental XRD and ND $T(r)$ data by this approach is shown in Figs. 4 and 5. The O–O peak at 0.28 nm, which belongs to the edges of the VO_n and ZnO_n polyhedra, may also be somewhat asymmetric. But the possibly existing tail on its right-hand side cannot be extracted. Only the main fraction of the O–O peak is obtained and, certainly, it cannot be separated from the continuous O–O correlations which may occur beyond 0.30 nm. All the detailed parameters of the fits are given in Table 2. The various Gaussian functions of the V–O and Zn–O peaks should not be interpreted as different species of V–O and Zn–O bonds or as different VO_n and ZnO_n polyhedra. The large number of fit parameters allows to approximate the peaks and their tails in the $T(r)$ data in excellent quality. Therefore, error bars are not given for most of the parameters in Table 2. But the uncertainties of the total coordination numbers and the mean distances are estimated (values given in parentheses). Only the V–O peak of v–V_2O_5 really indicates

Table 2. Parameters resulting from the Gaussian fit of the experimental X-ray and neutron correlation functions, $T(r)$, of v–V_2O_5 and of three zinc vanadate glasses (cf. Figs. 4 and 5) where the V–O and Zn–O first neighbor peaks are approximated by two to four Gaussian functions. * These parameters were fixed during the fits. ** These parameters of the third V–O and the second Zn–O Gaussian were taken to be equal. The distances and full widths at half maximum (fwhm) are given in nm.

Atom pair	Coordin. number	Distance	fwhm	Total coordination number	Mean distance
vitreous V_2O_5					
V–O	1.54	0.1640	0.019	4.8(2)	0.184(2)
	2.08	0.1830	0.017		
	0.82	0.2035	0.022		
	0.36*	0.2320*	0.030*		
O–O	6.00(15)	0.2750(20)	0.035(4)		
$(ZnO)_{0.2}(V_2O_5)_{0.8}$					
V–O	2.67	0.1690	0.022	4.5(2)	0.180(2)
	1.46	0.1885	0.024		
	0.36	0.2290**	0.058**		
Zn–O	4.21	0.2005	0.024	6.2(10)	0.210(5)
	1.96	0.2290**	0.058**		
O–O	6.14(15)	0.2775(20)	0.036(4)		
$(ZnO)_{0.4}(V_2O_5)_{0.6}$					
V–O	2.73	0.1695	0.018	4.2(2)	0.176(2)
	1.34	0.1875	0.027		
	0.10	0.2205**	0.040**		
Zn–O	3.96	0.1995	0.025	4.9(5)	0.203(3)
	0.91	0.2205**	0.040**		
O–O	5.86(15)	0.2795(20)	0.035(4)		
$(ZnO)_{0.5}(V_2O_5)_{0.5}$					
V–O	2.65	0.1700	0.018	4.2(2)	0.180(2)
	1.27	0.1890	0.029		
	0.32	0.2240**	0.033**		
Zn–O	3.83	0.2000	0.024	4.7(3)	0.204(2)
	0.90	0.2240**	0.033**		
O–O	5.67(15)	0.2800(20)	0.035(4)		

the existence of two different lengths of V–O bonds (cf. Figure 4).

The positions and the asymmetry of the Zn–O peaks do not change in dependence on the glass compositions (cf. Figure 5). The total Zn–O coordination numbers are about five. The uncertainty of N_{ZnO} of the glass with 20 mol% ZnO is too large to interprete the number of six (Table 2) as a real change. The V–O distances of the three modified glasses do not change, but the asymmetry of the peak and also N_{VO} increase from 4.2 to 4.5 in direction of the smaller ZnO fractions. Finally, a V–O coordination number of 4.8 is observed for v–V_2O_5, which is the same as observed before by Ag K_α radiation [16]. Two distances are visible (0.164 and 0.183 nm) where the second possesses more weight. The long tail

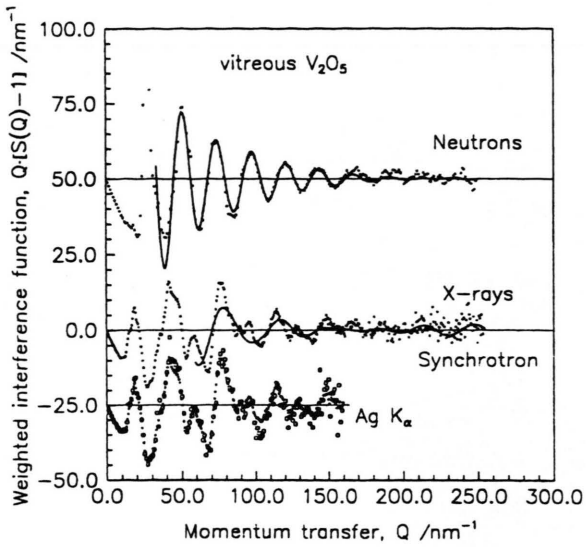

Fig. 6. Comparison of the experimental weighted interference functions, $Q \cdot [S(Q) - 1]$, of v–V_2O_5 obtained by neutrons and X-rays (dotted lines) with model functions calculated by the parameters of the V–O and O–O first-neighbor peaks given in Table 2 (solid lines). In the lower part of the plot, the data previously obtained by Ag K_α radiation from a conventional X-ray tube [16] (circles) are compared with the synchrotron data (dots). The upper and lower functions are shifted for clarity.

of V–O distances of v–V_2O_5 shows some small oscillations from 0.24 to 0.28 nm in the X-ray $T(r)$ function, which are not well approximated. They should not have any physical meaning.

4. Discussion

4.1. The Structure of Vitreous V_2O_5

In order to understand the structural behavior of the modified glasses it would be helpful to have detailed knowledge of the structure of v–V_2O_5. As already pointed out in Chapt. 1, v–V_2O_5 is hardly obtained even by quenching and its structure is still a matter of controversy [13–18, 29–31]. An origin of differences might be found in the preparation conditions. Nabavi et al. [18] gave an excellent survey of studies of v–V_2O_5 using the various methods which are sensitive to the structure. The present diffraction results agree with our previous data obtained by Ag K_α radiation with V–O coordination number, N_{VO}, also being 4.8 [16]. For illustration of the gain of information which is obtained by the high-energy photons of the synchrotron the weighted interference functions, $Q \cdot [S(Q) - 1]$, are compared in Figure 6.

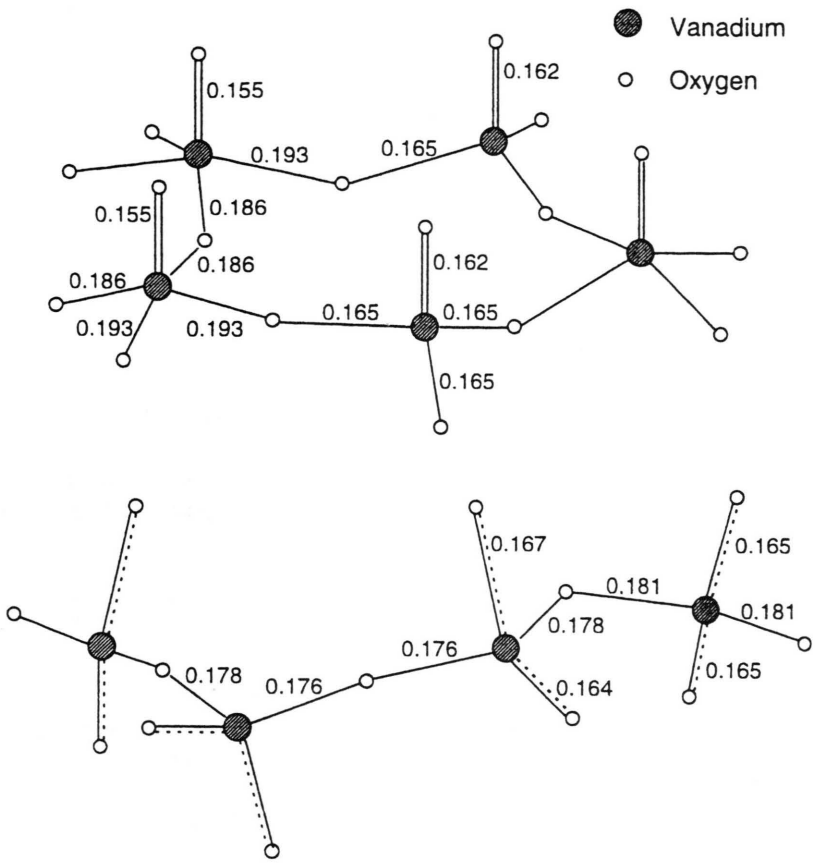

Fig. 7. A five-membered ring formed of VO_4 and VO_5 units taken from c–$K_3V_5O_{14}$ [33] and a chain segment of four VO_4 tetrahedra taken from c–$Ba(VO_3)_2$ [6]. Bond lengths are given in nm. Single lines denote single bonds, the double lines mark V=O double bonds and the dashed lines indicate the delocalization of the one V=O bond of a VO_4 unit onto its terminal V–O_T bonds. The bond lengths in the $K_3V_5O_{14}$ crystal [30] indicate the weakening of the V=O bond of the VO_4 unit due to a shift of electron density from an adjacent VO_5 of the VO_4 unit which also causes an elongation of the V–O_B bond of the VO_5 unit and a shortening of the V–O_B bond of the VO_4 unit.

Though further reduction of the noise of the synchrotron data is desirable, the additional information in the Q-range up to 250 nm^{-1} is responsible for the new details visible in the shape of the V–O peak (cf. Figure 4). The V–O first-neighbor distances can no more be fitted by a single Gaussian peak but three peaks at 0.164, 0.183, and 0.203 nm are necessary. Moreover, a flat tail accompanies the V–O peak which is approximateed by a fourth Gaussian. The model function of the X-ray $Q \cdot [S(Q) - 1]$ data (Fig. 6) results from the interference of several damped oscillations of different frequency which correspond to the various Gaussian peaks used for the approximation of the V–O and O–O first-neighbor distances. Some oscillations of rather short periods, which are visible between 150 and 200 nm^{-1}, are not approximated by this function. They are attributable to the effects of the strong V–V peak at 0.34 nm. A large range of the neutron data (Fig. 6) is well approximated by a single damped oscillation which is due to the strong O–O peak at 0.275 nm (cf. Figure 5).

The total V–O coordination number of v–V_2O_5, which includes also the tail of the V–O peaks, is 4.8 ± 0.2 (Table 2). This number could be interpreted with a network of VO_5 units which includes a minor fraction of VO_4 tetrahedra. Since 4.8 does not much differ from five, and since three V–O distances of 0.164, 0.183, and 0.203 nm are found (Table 2), also a structure similar to that of c–V_2O_5 [7, 32] could be assumed. However, as already pointed out in [16] the strong peak of V–V distances at 0.34 nm (cf. Fig. 4) contradicts the existence of a reasonable fraction of edge-connected VO_n units having shorter V–V separations, which are typical of the V_2O_5 crystal [7, 32]. Hence, the network structure of v–V_2O_5 is formed of VO_4 and VO_5 units, mainly linked by corners.

The V–O distances found between 0.21 and 0.30 nm are longer than those being typical of V–O bonds in compact VO_n polyhedra. In a first approach, such V–O distances should not be taken into account for identification of the network units. In several crystal structures,

e.g., c–$Zn(VO_3)_2$ [8] and c–V_2O_5 [7, 32] such longer distances exist where the VO_5 units can also be interpreted as very distorted VO_6 octahedra. Accordingly, if the flat tail of the V–O peak observed, i.e. the fourth Gaussian function at 0.232 nm, is assumed to be composed of such additional distances, then an N_{VO} of ≅4.4 instead of 4.8 has to be considered for estimation of the network units. This number indicates a mixture of equal amounts of VO_4 and VO_5 units forming the network of v–V_2O_5 such as found by ^{51}V NMR [18]. According to V–V distances of 0.34 nm, the VO_n units are mostly linked by corners. For stoichiometric reasons one terminal V=O double bond occurs per VO_4 unit, and due to the needs of charge compensation the V=O bond should be located in a VO_4 unit. Minor fractions of other structural features, such as three-coordinated O sites and edge-sharing VO_5 units with terminal V=O bonds, cannot be excluded. According to $N_{VO} = 4.4$, a fraction of 0.6 of VO_4 units with V=O bonds is expected. This number of V=O bonds is too small for the explanation of the fraction of short V–O bonds of 0.164 nm. A VO_4 unit having one terminal V=O bond is known for the $K_3V_5O_{14}$ crystal [33]. This VO_4 unit has single V–O bonds with lengths of 0.165 nm (cf. Figure 7). Thus, these bonds as well as all terminal V=O bonds contribute to the peak of the shorter V–O distances. The single V–O bonds of the VO_5 units in c–$K_3V_5O_{14}$ [33] have lengths of 0.186 and 0.193 nm, and they contribute to the peak of the longer V–O distances. Though the V–O peak in the $T(r)$ function of v–V_2O_5 (Fig. 4) is visibly composed of these two fractions, it is not feasible to separate the peak into these contributions. Asymmetric distributions of unknown shape would have to be taken into account for both fractions.

4.2. Structural Effects of the ZnO Additions

Strongest changes of the V–O distance peaks are found between the samples v–V_2O_5 and the 20 mol% glass, while less changes occur beyond 20 mol% ZnO content (cf. Figure 4). This behavior is confirmed by the N_{VO}'s and the mean r_{VO}'s when the tails, i.e. the flat Gaussian peaks at ≅0.23 nm, are not taken into account such as made for the numbers given in Table 3. Only the larger width (fwhm) of the first component of the V–O peak of the 20 mol% sample (Table 2) indicates already some changes toward that of v–V_2O_5. Thus, additions of ZnO do not change the structure of the vanadate glasses in a continous way, but the modification process itself is changed. At first, most of the VO_5 network units

Table 3. Total V–O coordination numbers and mean V–O distances calculated from the parameters of the Gaussian functions given in Table 2. Different from the data also given in Table 2, here the flat Gaussian peaks with distances of ≅0.23 nm are not taken into account. The distances are given in nm.

Sample	Total coordination number	Mean distance
v–V_2O_5	4.44(15)	0.180(2)
$x = 0.2$	4.13(10)	0.176(2)
0.4	4.07(10)	0.175(2)
0.5	3.92(10)	0.176(2)

are transformed to VO_4 tetrahedra, where N_{VO} decreases clearly. After 20 mol% ZnO only a small but significant decrease of N_{VO} exists with N_{VO} approaching about four at the metavanadate composition. The transition from a VO_5 to a VO_4 unit is accompanied by the formation of a terminal oxygen (O_T) site. Additionally, each ZnO leads to the breakage of a V–O_B–V bridge (bridging oxygen – O_B) with the formation of two O_T sites. Thus, a strong increase of the number of O_T sites accompanies the modification process near v–V_2O_5, while a smaller but continuous increase of the O_T fraction is developed beyond 20 mol% ZnO toward the metavanadate composition. Vanadate glasses of the latter range with compositions from 30 to 55 mol% MeO were studied by ^{51}V NMR spectroscopy, where the modifier oxides are CaO, SrO, and BaO [10]. No VO_5 units were found in the metavanadate glasses, but fractions of up to 25% VO_5 units were detected in glasses of 30 mol% MeO. This would correspond to an increase of N_{VO} from four in metavanadate glasses to 4.25 in glasses of 30 mol% MeO, which is little more than we observed, but the differences are in the limits or error. The behavior of the VO_4 units with the occurrence of branching, middle and end groups with three, two and one links per VO_4 unit is similar to that known of the phosphate glasses [11]. Additions of ZnO decrease the number of links between the VO_4 units. The V–O coordination number does not reflect this process. But the small decrease of N_{OO} indicates the decomposition of the networks because an O_T atom participates in a smaller number of edges of the network units than an O_B atom.

When studying the phosphate glasses by neutron diffraction experiments of high resolving power, two different P–O distances were observed [34, 35]. These two distances belong to the P–O_T and P–O_B bonds. In case of the present study of the vanadate glasses simi-

lar observations are not possible. The V–O correlations are not obtained by ND experiments and the XRD experiments with Q_{max}'s of 250 nm^{-1} are not sufficient to resolve the two distances (Q_{max} of about 400 nm^{-1} is required). Such a Q_{max} of 400 nm^{-1} becomes possible when scattering angles larger than those available at BW5 are used, where also the Compton scattering has to be suppressed [36]. But increased widths of the V–O_T and V–O_B components of the V–O peak if compared with those of the P–O bonds can make it impossible to separate the distances irrespective of any Q_{max}. Nevertheless, the two different lengths of V–O bonds are found if one analyses the bond lengths of the $Ba(VO_3)_2$ crystal [6] which is formed of only VO_4 middle groups. A chain segment of this crystal (cf. Fig. 7) illustrates this behavior. Thus, the concept of delocalization of the one P=O double bond of a PO_4 unit on all its P–O_T bonds [37] should also be valid for the VO_4 units. A detailed analysis of the P–O bonds of phosphate glasses containing mixtures of branching and middle PO_4 groups has shown [35] that the delocalization concept [37] acts in combination with the rules of structural variability [38] with electron shifts from the more negative middle groups to the branching units, which has consequences for the bond lengths. A similar behavior is effective between the VO_5 and VO_4 units of the $K_3V_5O_{14}$ crystal [33] (cf. Fig. 7) where negative charge is shifted from the VO_5 to the VO_4 unit. This shift is indicated [38] by an elongation of the V–O_B bond in the VO_5 unit and a shortening of the V–O_B bond in the VO_4 unit. Thus, changes in the neighborhood of the network units have effects on the lengths and the strengths of the bonds, which limits the possibility of the identification of the fractions of the network units when only poorly resolved peaks either in correlation functions or in vibration spectra are analysed on the basis of data of the related crystals.

Different from the phosphate glasses, a fraction of up to 40% VO_5 unit is found toward v–V_2O_5. Since a reasonable fraction of short V–V distances of about 0.31 nm is missing, edge-sharing links of the VO_5 units can play only a minor role. The V–V distance peak of v–V_2O_5 found at 0.34 nm broadens with increasing ZnO fractions (cf. Figure 4). Thus, the Zn–V separations have lengths of the same magnitude. Therefore, for the modified glasses edge-sharing VO_n units cannot be excluded by analysing the correlation functions. But VO_4 units sharing edges are not known of any vanadate crystal, and the fraction of VO_4 units increases with ZnO additions. It should not be assumed that the VO_5 units existing in the structure of the modified glasses share some edges if this behavior is not typical for v–V_2O_5 whose network has the highest fraction of VO_5 units. So the VO_5 units are suggested mostly to share corners with the neighboring VO_n polyhedra, where with increasing ZnO fractions also an O_T site can occur in the VO_5 unit.

The decrease of the V–O coordination number already beginning from v–V_2O_5 seems to contradict the behavior of the Ge–O coordination in the alkali germanate glasses [22, 39], whereby Ge–O and V–O bonds have similar lengths. In accordance with the formation of GeO_6 octahedra due to alkali additions one would expect the V atoms to increase their oxygen coordination number too, because a vanadium atom has an even higher valency. In contrast, a change of VO_5 to VO_4 units is detected with ZnO additions, whose origin is not understood. If one compares the crystal structures of c–$Zn(VO_3)_2$ [8] and c–$Ba(VO_3)_2$ [6], the larger Ba^{2+} cations prefer the formation of VO_4 units while the smaller Zn^{2+} cations fit a structure with zig-zag chains of edge-sharing VO_5 units. Each of the VO_4 and VO_5 units has two O_T sites. In the crystal the Zn^{2+} cations are coordinated with six oxygens while N_{ZnO} is about five in the vanadate glasses (cf. Table 2). Smaller Zn–O coordination numbers indicate more open structures which would be equivalent with the situation of larger modifier cations. Thus, it is suggested that the networks formed of VO_4 instead of VO_5 units are more suitable to accommodate larger Me^{2+} cations and also higher MeO fractions.

It was already mentioned that the V–V and Zn–V distances are similar. Thus, it would be interesting to study the medium-range order of this system where VO_n polyhedra are replaced by ZnO_n polyhedra. No clear changes of the first diffraction peaks in the $S_X(Q)$ data are observed in dependence on the ZnO fraction (cf. Figure 1). An analysis of the medium-range order is planned together with some modelling. Here only the local environments of Zn^{2+} cations are discussed. The Zn–O peak is approximated by two Gaussian functions, where for all three modified glasses studied a first Zn–O distance of 0.200 nm is obtained with about four oxygen neighbors. The second distance approximates the tail of this asymmetric peak and is fitted by a Gaussian at 0.22 to 0.23 nm with one further oxygen. This tail yields a larger contribution only in

case of the 20 mol% ZnO glass, where due to the small ZnO fraction the uncertainty of the determination of parameters of the Zn–O peak is higher. Thus, the increase to about six for N_{ZnO} of the 20 mol% glass is not significant. Different from the $(ZnO)_x(P_2O_5)_{1-x}$ glasses, where a decrease of N_{ZnO} from six for $x = 0.33$ to four for $x = 0.5$ is observed accompanied by a decrease of r_{ZnO} from 0.205 to 0.195 nm [19, 20], in the vanadate glasses no change of the Zn–O coordination with N_{ZnO} of five and r_{ZnO} of $\cong 0.204$ nm is observed. In the phosphate glasses this change was attributed to effects of the number of O_T sites available for each Zn^{2+} cation. Several reasons may reduce such effects in the vanadate glasses: The number of O_T sites is smaller when VO_5 units are formed. The VO_5 units coexisting with the VO_4 branching units in glasses of $x < 0.5$ give an additional degree of freedom for the network formation which supplies a better way for the distribution of charges. VO_5 units have nearly the same dimensions as the ZnO_5 polyhedra. Finally, also the few V^{4+} atoms may occupy those octahedral sites which, otherwise, would be occupied by a Zn^{2+} cation. Thus, the high flexibility of the vanadate networks if compared with a phosphate network allows the Zn^{2+} cations to form 'convenient' environments which have not to be changed in dependence on the ZnO fraction.

5. Conclusions

X-ray diffraction experiments are more important than neutron diffraction one, when the structure of vanadate glasses is studied. For a detailed discussion of the V–O coordination it is desirable to use a measuring range with a Q_{max} clearly larger than 200 nm^{-1}. The V–O and Zn–O first-neighbor peaks of the three $(ZnO)_x(P_2O_5)_{1-x}$ glasses studied with $x = 0.2$, 0.4, and 0.5 are asymmetric and cannot be approximated by single Gaussian functions. The V–O peak of vitreous V_2O_5 is composed of two visible components which can be attributed to different bond lengths in VO_4 and VO_5 units. Also the V–O coordination number of 4.4 of this glass indicates the coexistence of both groups. All VO_n polyhedra are dominantly linked by corners. ZnO additions reduce the fraction of VO_5 units, so that at the metavanadate composition ($x = 0.5$) only VO_4 tetrahedra preferably forming chains are left. The strongest decrease of the fraction of VO_5 units is found for $x < 0.2$. The Zn–O coordination numbers of all three modified glasses are about five with closest distances of $\cong 0.200$ nm.

Acknowledgements

Financial support of Deutsche Forschungsgemeinschaft (contract KR 1372/7-1) is gratefully acknowledged.

[1] M. Sayer and A. Mansingh, Phys. Rev. B **6**, 4629 (1972).
[2] A. Ghosh, Phys. Rev. B **42,** 5665 (1990).
[3] N. F. Mott, J. Non-Cryst. Solids **1,** 1 (1968).
[4] S. Sen and A. Ghosh, J. Non-Cryst. Solids **258,** 29 (1999).
[5] S. Sen and A. Ghosh, J. Phys.: Condens. Matter **11,** 1529, (1999).
[6] T. Yao, Y. Oka, and N. Yamamoto, Inorg. Chimica Acta **238,** 165 (1995).
[7] J. A. A. Ketelaar, Nature (London) **137,** 316 (1936).
[8] G. D. Andreetti, G. Calestani, A. Montenero, and M. Bettinelli, Z. Kristallogr. **168,** 53 (1984).
[9] R. Gopal and C. Calvo, Canadian J. Chem. **51,** 1004 (1973).
[10] S. Hayakawa, T. Yoko, and S. Sakka, J. Ceram. Soc. Japan **102,** 530 (1994).
[11] J. R. Van Wazer, Phosphorus and its Compounds, vol. 1, Interscience, New York 1958.
[12] Y. Dimitriev, V. Dimitrov, M. Arnaudov, and D. Topalov, J. Non-Cryst. Solids **57,** 147 (1983).
[13] A. Mosset, P. Lecante, J. Galy, and J. Livage, Phil. Mag. B **46,** 137 (1982).
[14] H. Morikawa, M. Miyake, S.-I. Iwai, K. Furukawa, and A. Revcolevschi, J. Chem. Soc. Faraday Trans. I **77,** 361 (1981).
[15] M. Seshasayee and K. Muruganandam, Solid State Commun. **105,** 243 (1998).
[16] U. Hoppe, R. Kranold, and E. Gattef, Solid State Commun. **108,** 71 (1998).
[17] U. Hoppe and R. Kranold, Solid State Commun. **109,** 625 (1999).
[18] M. Nabavi, C. Sanchez, and J. Livage, Phil. Mag. B **63,** 941 (1991).
[19] U. Hoppe, G. Walter, R. Kranold, D. Stachel, and A. Barz, J. Non-Cryst. Solids **192–193,** 28 (1995).
[20] U. Hoppe, G. Walter, D. Stachel, A. Barz, and A. C. Hannon, Z. Naturforsch. **52a,** 259 (1997).
[21] U. Hoppe, J. Non-Cryst. Solids **195,** 138 (1996).
[22] U. Hoppe, R. Kranold, H.-J. Weber, J. Neuefeind, and A. C. Hannon, J. Non-Cryst. Solids **278,** 99 (2000).
[23] H. F. Poulsen, J. Neuefeind, H.-B. Neumann, J. R. Schneider, and M. D. Zeidler, J. Non-Cryst. Solids **188,** 63 (1995).
[24] J. H. Hubbell, Wm. J. Veigele, E. A. Briggs, R. T. Brown, D. T. Cromer, and R. J. Howerton, J. Phys. Chem. Ref. Data **4,** 471 (1975).
[25] Y. Waseda, in: The Structure of Non-Crystalline Materials, McGraw-Hill, New York 1980, p. 11 ff.
[26] A. C. Hannon, W. S. Howells, and A. C. Soper, IOP Conf. Series **107,** 193 (1990).
[27] A. J. Leadbetter and A. C. Wright, J. Non-Cryst. Solids **7,** 23 (1972).
[28] D. Marquardt, SIAM J. on Appl. Math. **11,** 431 (1963).

[29] Y. Dimitriev and V. Dimitrov, Mater. Res. Bull. **13,** 1071 (1978).
[30] S. Takeda, Y. Kawakita, M. Inui, K. Maruyama, S. Tamaki, K. Sugiyama, and Y. Waseda, J. Non-Cryst. Solids **205–207,** 151 (1996).
[31] Y. Kawakita, H. Nakashima, S. Yoshioka, S. Takeda, K. Marayama, M. Inui, and K. Tamura, J. Phys. Chem. Solids **60,** 1483 (1999).
[32] R. Enjalbert and J. Galy, Acta Crystallogr. C **42,** 1467 (1986).
[33] A. M. Bystroem and H. T. Evans, Acta Chem. Scand. **13,** 377 (1959).
[34] U. Hoppe, G. Walter, R. Kranold, and D. Stachel, J. Non-Cryst. Solids **263–264,** 29 (2000).
[35] U. Hoppe, R. Kranold, D. Stachel, A. Barz, and A. C. Hannon, Z. Naturforsch. **55a,** 369 (2000).
[36] V. Petkov, S. J. L. Billinge, S. D. Shastri, and B. Himmel, Phys. Rev. Lett. **85,** 3436 (2000).
[37] R. K. Brow, J. Non-Cryst. Solids **263–264,** 1 (2000).
[38] V. Gutmann, in The Donor – Acceptor Approach to Molecular Interactions, Plenum Press, New York 1978, pp. 4–16.
[39] H. Verweij and J. H. J. M. Buster, J. Non-Cryst. Solids **34,** 81 (1979).